Hyperfine Interact
DOI 10.1007/s10751-013-0767-z

Formation of magnetic nanoparticles studied during the initial synthesis stage

M. Kraken · I.-C. Masthoff · A. Borchers · F. J. Litterst · G. Garnweitner

Abstract The formation of iron oxide nanoparticles in course of a sol-gel preparation process was traced by UV/Vis and ^{57}Fe Mössbauer absorption spectroscopy. Samples were extracted at different stages of the reaction. While spectra measured on samples extracted at low reactor temperatures showed the starting materials Fe(acac)$_3$ diluted in benzyl alcohol undergoing slow paramagnetic relaxation, a sample extracted at a reactor temperature of 180 °C gave clear evidence for emerging iron oxide nanoparticles. A prolonged stay at 200 °C results in a complete transformation from Fe(acac)$_3$ to maghemite nanoparticles.

Keywords Non-aqueous sol-gel method · Mössbauer spectroscopy · Spin-spin relaxation

1 Introduction

The scientific interest in magnetic nanoparticles has increased continuously over the last years, resulting from their distinct physical properties leading to numerous technological applications [1]. A reproducible preparation technique, yielding

---

Thirteenth Latin American Conference on the Applications of the Mössbauer Effect, LACAME 2012, Medellín, Columbia, 11–16 November 2012.

M. Kraken (✉) · A. Borchers · F. J. Litterst
Institut für Physik der kondensierten Materie, Technische Universität Braunschweig,
Mendelssohnstrasse 3, 38106 Braunschweig, Germany
e-mail: m.kraken@tu-bs.de

I.-C. Masthoff · G. Garnweitner
Institut für Partikeltechnik, Technische Universität Braunschweig,
Volkmaroder Str. 5, 38104 Braunschweig, Germany

monodisperse, spherical particles is essential, since the physical properties of the particles strongly depend on these features. The non-aqueous sol-gel method is a bottom-up synthesis that allows preparation of particles with the desired properties. For this method, a precursor is dispersed in a high-boiling, organic solvent and following heat-up, the reaction is left to proceed for a variable span of time. Our aim is, to monitor the thermal decomposition of $Fe(acac)_3$ in benzyl alcohol (BA) and triethylene glycol (TEG) in order to gain an understanding about the formation of the magnetic nanoparticles. Based on the system described in [2], we performed further measurements to enlarge our knowledge of this synthesis route. This work focuses on the heat-up phase to 200 °C in a reactor using BA as solvent. Samples taken during the heating up process, as well as the mixed starting materials are discussed. Details about the reaction after reaching 200 °C and a comparison to TEG as a solvent will be presented elsewhere.

2 Experimental

Synthesis of magnetic nanoparticles The iron oxide nanoparticles were synthesized in a 1.5 L reactor (Polyclave, Typ 3/1 Büchi Glas Uster) using $Fe(acac)_3$ as only iron source and benzyl alcohol as solvent [2]. In a typical procedure the reactor was filled with 50 g $Fe(acac)_3$ and 1 L solvent and the reaction was left to proceed whilst stirring at 200 °C for 23 h. Samples were taken every 20 °C during the heating process and immediately cooled to room temperature (RT) in an ice bath. In the following, the reactor temperature at which the sample was taken will be called T_R. The samples were used for analysis without any further modifications.

For the ultraviolet-visible spectrophotometry (UV/Vis) the UV-3100PC Spectrophotometer from VWR is used, the samples being measured in a wavelength range from 300 to 500 nm.

^{57}Fe Mössbauer absorption measurements were performed on a standard spectrometer using a ^{57}CoRh source in a temperature range from 4 to 300 K. Absorbers were prepared from samples drawn from the reactor by rapidly cooling them to 80 K.

3 Results and discussion

The UV/Vis spectra, shown in Fig. 1, obtained for the samples taken during the heating process display the conversion of the precursor iron(III) acetylacetate in BA to Fe_2O_3 nanoparticles, being described by

$$\mathrm{Fe(acac)_3} \xrightarrow{\textit{solvolysis}} \mathrm{Fe(OH)_{3-x}(OR)_x} \xrightarrow{\textit{condensation}} \mathrm{Fe_2O_3}.$$

Spectra taken from samples between $T_R = \mathrm{RT}$ up to 140 °C show two distinct adsorbance maxima at the wavelengths 440 nm and at 360 nm. The absorbance is typical for $Fe(acac)_3$ [3]. For the samples taken above 180 °C the absorbance at 440 nm decreases reaching a constant value of 1.1. By comparing these curves, it is concluded that at a temperature of 180 °C the conversion from $Fe(acac)_3$ to iron oxide nanoparticles sets in.

Fig. 1 UV/Vis spectra for $Fe(acac)_3$ dissolved in BA taken from the reactor at different temperatures

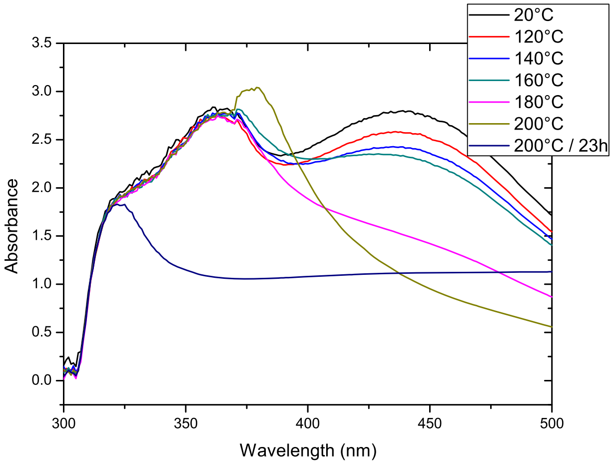

Fig. 2 Mössbauer spectra of $Fe(acac)_3$ dispersed in BA with a concentration of 50 g/L measured at 20 K and 80 K for $T_R = \text{RT}$. The parameters of the fit to the measurement at 20 K can be found in Table 1

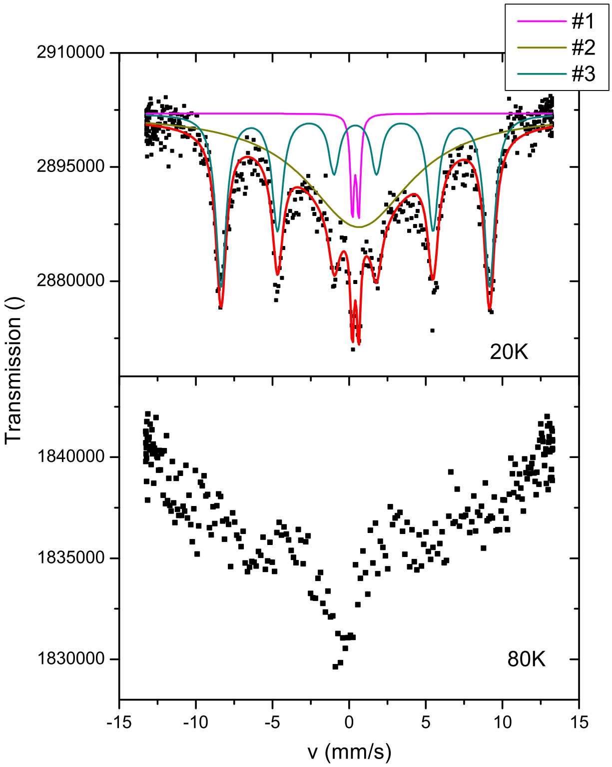

In order to gain more information about this transformation, we performed ^{57}Fe Mössbauer absorption measurements. In a first step, we examined a sample extracted from the reactor at $T_R = \text{RT}$, i.e. directly after preparing the solution. The spectra are shown in Fig. 2. At low temperatures, a well-resolved sextet with

Table 1 Parameters of the spectra shown in Fig. 3: centershift CS relative to metallic Fe at RT, magnetic hyperfine field B_{hyp}, quadrupole splitting $e^2qQ/2$, linewidth W (HWHM) and the relative spectral area

T_R (°C)	#	CS (mm/s)	B_{hyp} (T)	$e^2qQ/2$ (mm/s)	W (mm/s)	Area (%)
RT	1	0.52	0.00	0.42	0.14	4
RT	2	0.74	0.00	0.00	4.15	60
RT	3	0.51	54.3	0.00	0.42	36
160	1	0.51	0.00	0.50	0.19	9
160	2	0.51	0.00	0.00	3.58	55
160	3	0.52	54.3	0.01	0.32	36
180	1	0.51	0.00	0.45	0.16	16
180	2	0.44	0.00	0.00	5.68	33
180	3	0.54	54.4	−0.03	0.27	8
180	4	0.45	46.3	0.01	0.56	43
200/30 min	4	0.43	50.4	0.00	0.41	100

The site numbers in the second column are given in the same color as the corresponding subspectra in Fig. 2 (T_R =RT), Fig. 3 ($T_R = 160$ °C and $T_R = 180$ °C) and Fig. 4 (after 30 min at 200 °C)

a broad background and a non-magnetic doublet component can be observed (fit parameters are given in Table 1). With increasing absorber temperature, the sextet broadens and the background fraction increases. The magnetic hyperfine splitting at 20 K corresponds to a magnetic hyperfine field of $B_{\mathrm{hyp}} \sim 54.3$ T. The magnitude of the magnetic hyperfine field as well as the temperature dependent collapse of the sextet could in principle be interpreted with the typical behavior of superparamagnetic, well crystallized magnetic nanoparticles. However, since the UV/Vis measurements only indicate the formation of magnetic nanoparticles for reactor temperatures far above RT, superparamagnetic particles cannot be the origin of these spectra.

Therefore the spectra shown in Fig. 2 need to be interpreted in a different way. As has been demonstrated already in the very early days of Mössbauer spectroscopy, dilute $\mathrm{Fe(acac)_3}$ in an organic solvent [4] reveals very similar spectra at low temperatures. Also the magnetic hyperfine splitting reported in [4] is in good agreement with our data. Reason for the apparent magnetic hyperfine splitting is the strong suppression of spin-spin relaxation between the relatively distant $\mathrm{Fe^{III}}$. In this case the hyperfine patterns are determined by the coupling of the nuclear spin with the electronic ground state spin of high-spin $S = 5/2$ in a weak axial crystalline electric field. Whereas the $|S_z = \pm 5/2\rangle$ and $|S_z = \pm 3/2\rangle$ Kramers doublets lead to sextet patterns, the $|S_z = \pm 1/2\rangle$ doublet results in a more complex and broad structure since relaxational fluctuations within this electronic state are still finite even at low temperature (see, e.g., [5]). Therefore the magnetic hyperfine structure visible in Fig. 2 is not related to the formation of magnetic nanoparticles, but is characteristic of the frozen solution of $\mathrm{Fe(acac)_3}$ and thus is also not in contradiction to our conclusions drawn from the UV/Vis spectra.

We want to note that the simplistic fit strategy used here (comprising a sextet, a broad background and a doublet) is inadequate for a proper description for the slow dynamic hyperfine patterns. It only shall be used for a rough estimate of the hyperfine parameters.

Fig. 3 Mössbauer spectra measured at 15 K for the solutions with $T_R = 160\,°\mathrm{C}$ and $T_R = 180\,°\mathrm{C}$

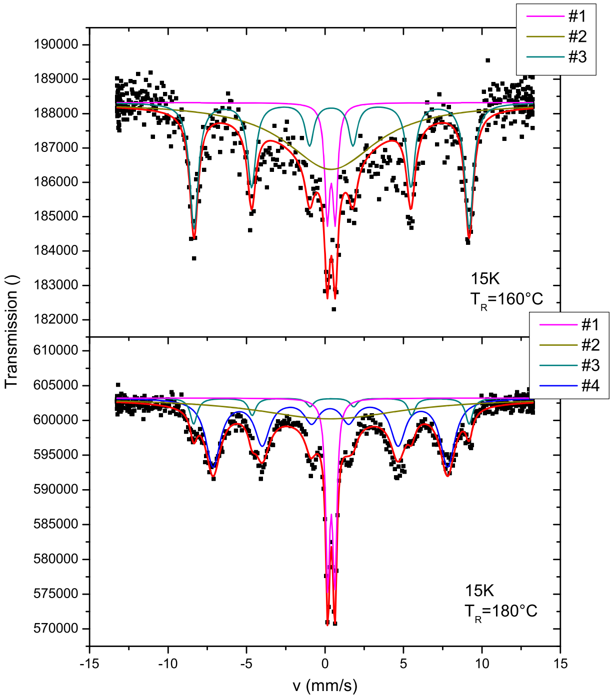

A discussion regarding the origin of the sharp doublet patterns visible in Fig. 2 will follow below.

The Mössbauer spectra for samples extracted at $T_R = 160\,°\mathrm{C}$ and for $T_R = 180\,°\mathrm{C}$ and measured at 15 K are shown in Fig. 3, the corresponding parameters in Table 1. The spectrum for $T_R = 160\ °\mathrm{C}$ exhibits a similar structure like the 20 K spectrum in Fig. 2 it can be fitted with the same strategy. The Mössbauer spectrum for $T_R = 180\ °\mathrm{C}$ was fitted including an additional sextet with a magnetic hyperfine field of 46.3 T. In accordance with the UV/Vis data, this sextet is interpreted as resulting from the emerging ferrite nanoparticles. The hyperfine field is smaller compared to the typical hyperfine field of nanoscaled ferrite particles ($\sim$52 T for maghemite [6]). This can be explained by an increased amount of spin canting within the particles due to the yet poor crystallinity, as may also be seen from the broad line width W.

The area of the doublet in the $T_R = 180\ °\mathrm{C}$ spectrum is bigger than the area of the doublet in the spectrum for $T_R = 160\ °\mathrm{C}$. We attribute this doublet to an intermediate stage in the development of particles, where agglomerates, comprising several Fe-ions are formed. The distance between individual $\mathrm{Fe}^{\mathrm{III}}$-ions in these agglomerates becomes shorter than in the completely dilute solution. Therefore, paramagnetic relaxation is enhanced. For relaxation frequencies higher than the nuclear Larmor precession frequency, the magnetic hyperfine splitting collapses into a non-magnetic doublet pattern. This is the same doublet as the one observed in Fig. 2 and it indicates that already the start solution ($T_R = \mathrm{RT}$) contains a small amount of these aggregates. Figure 4 shows the temperature dependent spectra of a sample extracted after reaching the final temperature of 200 °C and staying at this

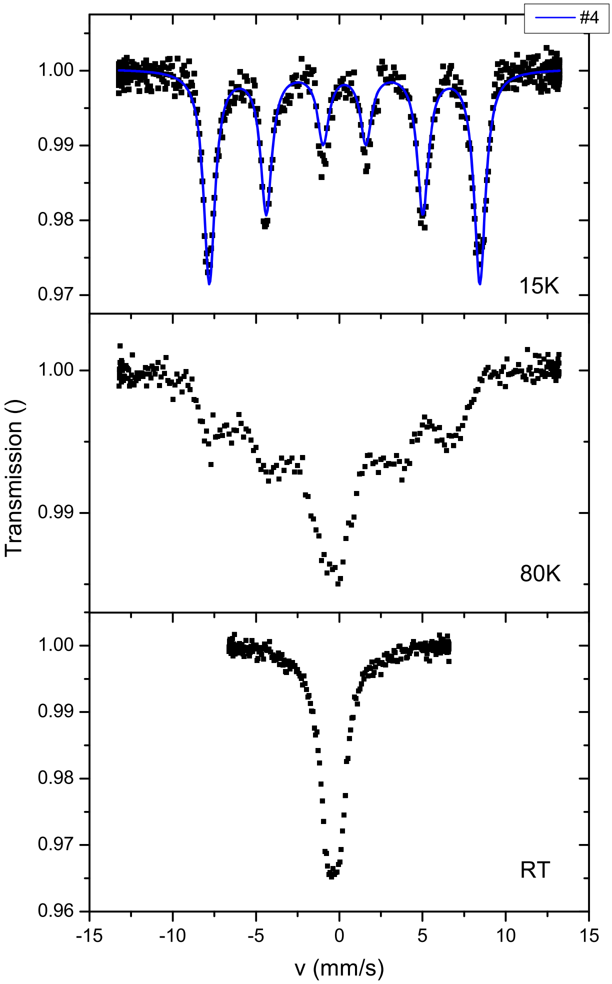

Fig. 4 Temperature dependent Mössbauer spectra of a sample extracted after staying at $T_R = 200$ °C for 30 min. The fit parameters for the measurement at 15 K can be found in Table 1

temperature for 30 min. The spectra are now typical for nanocrystalline maghemite. No relicts of the subspectra #1, 2 and 3 found at lower T_R can be traced. However, the crystallinity of the nanoparticles is still rather poor, as indicated by the magnetic hyperfine field with a value of ~50.4 T, which is smaller than the value for well-crystallized maghemite. The magnetic freezing temperature is about 80 K.

4 Conclusion

We investigated the formation of iron oxide nanoparticles during the initial synthesis stage by means of UV/Vis spectroscopy and Mössbauer spectroscopy. While the spectra of samples extracted at low reactor temperatures T_R up to 160 °C were typical for dilute $\mathrm{Fe(acac)_3}$ in solution undergoing slow paramagnetic relaxation, the measurements at $T_R = 180$ °C gave clear evidence for emerging magnetic nanoparticles.

Prolonged reaction at 200 °C yields formation of maghemite particles, that still are not well crystallized as can be seen from the reduced value of the magnetic hyperfine field. The gradual growth and improvement of crystallinity of the nanoparticles and its dependence on solvents will be presented elsewhere.

References

1. Frey, N.A., Peng, S., Cheng, K., Sun, S.: Magnetic nanoparticles: synthesis, functionalization, and applications in bioimaging and magnetic energy storage. Chem. Soc. Rev. **38**, 2532–2542 (2009)
2. Grabs, I.-M., Bradtmöller, C., Menzel, D., Garnweitner, G.: Formation mechanism of iron oxide nanoparticles in different nonaqueous media. Cryst. Growth Des. **12**, 1469–1475 (2012)
3. Muhammad, A.: Lewis Acidity of Tris(acetylacetonate) iron (III) Interactions with some Phosphine Derivative in Methylene Chloride Solution. J. Chem. Soc. Pak. **14**, 88 (1992)
4. Wignall, J.W.G.: Mössbauer line broadening in trivalent iron compounds. J. Chem. Phys. **44**, 2462 (1966)
5. Wickman, H.H., Wertheim, G.K.: Spin relaxation in solids and aftereffects of nuclear transformations. In: Goldankii, V.I., Herber, R.H. (eds.) Chemical Applications of Mössbauer Spectroscopy, chapter 12. Academic Press, London (1968)
6. Serna, C.J., Bødker, F., Mørup, S., Morales, M.P., Sandiumenge, F., Veintemillas-Verdaguer, S.: Spin frustration in maghemite nanoparticles. Solid State Commun. **118**, 437–440 (2001)